Solvent effects on the sodium borohydride reduction of 2-halocyclohexanones

Rodrigues Silva, Daniela; Zeoly, Lucas A.; Vermeeren, Pascal; Cormanich, Rodrigo A.; Hamlin, Trevor A.; Fonseca Guerra, Célia; Freitas, Matheus P.

published in
Journal of Physical Organic Chemistry
2023

DOI (link to publisher)
10.1002/poc.4556

document version
Publisher's PDF, also known as Version of record

Received: 3 April 2023 | Revised: 1 June 2023 | Accepted: 20 June 2023

DOI: 10.1002/poc.4556

RESEARCH ARTICLE

Journal of Physical Organic Chemistry WILEY

Solvent effects on the sodium borohydride reduction of 2-halocyclohexanones

Daniela Rodrigues Silva[1,2] | **Lucas A. Zeoly**[3] | **Pascal Vermeeren**[1] | **Rodrigo A. Cormanich**[3] | **Trevor A. Hamlin**[1] | **Célia Fonseca Guerra**[1] | **Matheus P. Freitas**[2]

[1]Department of Theoretical Chemistry, Amsterdam Institute of Molecular and Life Sciences (AIMMS), Amsterdam Center for Multiscale Modeling (ACMM), Vrije Universiteit Amsterdam, Amsterdam, the Netherlands

[2]Department of Chemistry, Institute of Natural Sciences, Federal University of Lavras, Lavras, Minas Gerais, Brazil

[3] Chemistry Institute, University of Campinas, Campinas, São Paulo, Brazil

Correspondence
Matheus P. Freitas, Department of Chemistry, Institute of Natural Sciences, Federal University of Lavras, 37200-900 Lavras, Minas Gerais (Brazil).
Email: matheus@ufla.br

Funding information
Coordenação de Aperfeiçoamento de Pessoal de Nível Superior, Grant/Award Number: 001; Conselho Nacional de Desenvolvimento Científico e Tecnológico, Grant/Award Number: 306830/2021-3; Fundação de Amparo à Pesquisa do Estado de Minas Gerais, Grant/Award Number: APQ-00383/15; Fundação de Amparo à Pesquisa do Estado de São Paulo, Grant/Award Number: 2018/03910-1; Fundo de Apoio ao Ensino, Pesquisa e Extensão, Grant/Award Number: 2466/20; Netherlands Organization for Scientific Research

Abstract

We have investigated the stereoselectivity and reactivity of the sodium borohydride reduction of 2-X-cyclohexanones (X=H, Cl, Br) using a combined approach of competitive experiments and density functional theory calculations. Our results show that the hydride addition proceeds via a late transition state in which the C–H bond is nearly formed, consistent with the mild reducing power of $NaBH_4$. The reaction barrier decreases from the 2-halocyclohexanones to the unsubstituted cyclohexanone, in line with relative reactivities observed in the competitive experiments. Furthermore, we provide a protocol to solve the longstanding issue of properly modelling the axial–equatorial facial selectivity of hydride addition to the carbonyl group substituted with a vicinal polar group. The inclusion of implicit solvation in combination with an explicit solvent molecule is crucial to reproduce the stereoselective formation of the *cis* product observed experimentally.

KEYWORDS

density functional computations, halogens, reactivity, solvation, stereoselectivity

1 | INTRODUCTION

The stereoselectivity of nucleophilic addition to carbonyl groups bonded to asymmetric centres has intrigued chemists for nearly three-quarters of a century.[1] Depending on the nature and arrangement of the groups on the prochiral carbon, the nucleophilic attack to one face of the carbonyl group may be preferred over the other.[2] To explain this selectivity, several models have been proposed over the years, which are based on effects

such as steric hindrance,[3] chelation,[4] polarization,[5] conformational stability,[6] torsional strain,[7] antiperiplanar orbital interactions,[8] and electrostatics.[9]

The hydride addition of small nucleophiles (such as $LiAlH_4$ or $NaBH_4$) to conformationally biased cyclohexanones is known to preferentially occur to the axial face (that leads to the equatorial alcohol) rather than to the equatorial face (that results in the axial alcohol; see Scheme 1).[10] This is counter to the reasoning based on steric arguments, as the axial face is more sterically hindered because of the axial hydrogens in the cyclohexanone backbone. The most accepted rationale to explain the preference for the axial attack is based on the model developed by Felkin[7] and later supported by Anh and Eisenstein,[8a] the so-called Felkin–Anh model. According to this model, addition to the equatorial face experiences more (destabilizing) torsional strain than to the axial face because of the eclipsing interaction with vicinal bonds (Scheme 1). Furthermore, the axial addition has the C–H bond antiperiplanar to the incoming nucleophile, leading to a stabilization of the transition state (TS) due to the $\sigma_{C-Nu} \rightarrow \sigma^*_{C-H}$ charge transfer.[11]

The validity of the Felkin–Anh model, however, to describe the stereoselectivity in cases of polar substituted ketones, such as 2-fluoroketones, has been questioned in the literature.[12] It is argued that the preferential formation of the *cis* diastereoisomer can be ascribed to the conformational stability of the original ketone.[13] That is, the *cis*:*trans* ratio increases as X goes from F to I (i.e., from 70:30 to 100:00, respectively) because the stability of the axial conformer, which places the halogen atom antiperiplanar to the hydride addition, increases in the same direction (Scheme 2).[14] The lower reactivity of the reduction of some 2-fluoroketones, compared with the chloro and bromo derivatives, has also been associated with their conformational preferences.[15] A remarkable

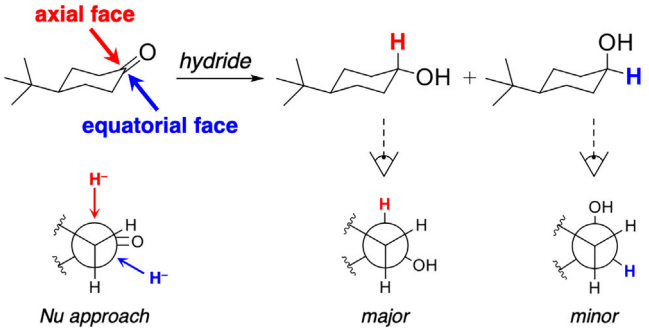

SCHEME 1 Hydride reduction of 4-*tert*-butylcyclohexanone via axial and equatorial addition to the carbonyl group, which leads to the formation of the corresponding equatorial and axial alcohol, respectively. For small hydrides, such as $LiAlH_4$ and $NaBH_4$, the equatorial alcohol is the major product.

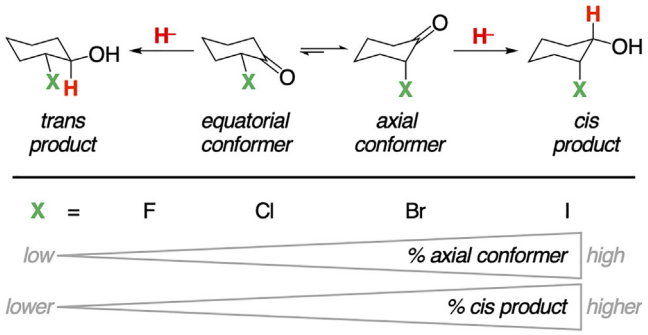

SCHEME 2 Conformational equilibrium of 2-halocyclohexanones and their respective hydride reduction.

implication is that rational modifications aiming at inducing specific conformational changes could be used to modulate the rates of a reaction. Nevertheless, attempts to theoretically model the stereoselectivity of hydride reduction of 2-substituted cyclohexanones with polar groups have been challenging.[16,17]

We have investigated the hydride addition to 2-X-cyclohexanones (X=H, Cl, Br) using competitive experiments and density functional theory computations. The main goal is to obtain insights into the reactivity and stereoselectivity of the hydride reduction of 2-halocyclohexanones (i.e., X=Cl, Br) by $NaBH_4$, whose reaction mechanism has been less explored than that of the $LiAlH_4$ reduction. The reaction mechanism studied in our work is inspired by the general reduction mechanism that is well-established in the literature.[11,16–18] For comparison purposes, the unsubstituted cyclohexanone (i.e., X=H) is used as a baseline. We also discuss to what extent the reaction mechanism is influenced by a polar solvent (i.e., ethanol) and that the inclusion of an explicit solvent molecule is essential to recover the experimentally observed stereoselectivities.

2 | METHODS

2.1 | Experimental section

2.1.1 | Competitive experiments of 2-X-cyclohexanone reduction with $NaBH_4$

In a 10.0 mL round bottom flask, 1.0 equiv. of cyclohexanone (24.9 mg, 0.25 mmol), 1.0 equiv. of 2-chlorocyclohexanone (33.7 mg, 0.25 mmol) and 1.0 equiv. 2-bromocyclohexanone (45.0 mg, 0.25 mmol) were added. This mixture was dissolved in 2.54 mL of absolute ethanol (0.1 mol L^{-1}), and the solution was vigorously stirred using a magnetic bar. To this solution, 0.2 equiv. of $NaBH_4$ (1.9 mg, 0.51 mmol) were added in a single

portion, and the reaction was stirred for 30 min. A substoichiometric amount of hydride was used to observe ketone peaks and measure the relative proportion of products formed. After that, the reaction was quenched with saturated NH_4Cl solution (2 mL) and was extracted with ethyl acetate (5 × 2 mL). Aliquots from the combined organic fractions were directly analysed by gas chromatography–flame ionization detection (GC–FID) and GC–mass spectrometry (GC–MS) using an HP-5MS column (30 m, 0.25 mm, 0.25u) in both equipment. The relative amount of product formed was obtained by integration of the area of its corresponding peak in the GC–FID chromatogram. The nuclear magnetic resonance (NMR) spectra were acquired at 500 MHz for ^{1}H and 125 MHz for ^{13}C, from ~20 mg cm^{-3} $CDCl_3$ solution. The results are provided in Figures S1–S6.

2.2 | Computational details

All calculations were performed using the Amsterdam Density Functional (ADF2017.103) software package.[19] Geometries and energies were calculated at the BLYP level of the generalized gradient approximation (GGA); exchange functional developed by Becke (B), and the GGA correlation functional developed by Lee, Yang and Parr (LYP).[20] The BLYP functional has been previously shown to yield correct trends in reactivity for a diverse set of organic reactions.[21] Scalar relativistic effects were accounted for using the zeroth-order regular approximation (ZORA).[22] Molecular orbitals (MO) were expanded in a large uncontracted set of Slater-type orbitals (STOs) containing diffuse functions: TZ2P.[23] The basis set is of triple-ζ quality and is augmented with two sets of polarization functions on each atom. To speed up the computations, the core shells of the atoms (i.e., 1 s for B, C, O and Na; and up to 2p for Cl) were treated by the frozen core approximation. Solvent effects using ethanol were accounted for in two ways, namely, implicit solvation and microsolvation. Implicit ethanol solvation was approximated using the conductor-like screening model (COSMO),[24] a dielectric model in which the molecular system is embedded in a cavity surrounded by a dielectric medium with given dielectric constant (for ethanol, $\varepsilon = 24.5$). On the other hand, microsolvation is referred herein as the approach in which solvent effects are taken into account as implicit solvation in combination with one explicit solvent molecule. The position and number of explicit solvent molecules was based on the ab initio molecular dynamic simulation study of Tomoda and coworkers,[25] in which they reported that there are up to three solvent molecules coordinated with the sodium atom, whereas only one simultaneously coordinates to the substrate via hydrogen bonding. The latter has been included in our microsolvated computations. The accuracies of the fit scheme (ZLM fit)[26] and the integration grid (Becke grid)[27] were set to 'very good'. In addition, trends in reactivity and stereoselectivity are unchanged when the dispersion correction was included[28] at COSMO (ethanol)-ZORA-BLYP-D3(BJ)/TZ2P//COSMO (ethanol)-ZORA-BLYP/TZ2P (Tables S1 and S2) or without the dispersion correction at COSMO (ethanol)-ZORA-BLYP/TZ2P. All stationary points were confirmed to be true minima (no imaginary frequencies) or TSs (one imaginary frequency) through vibrational analyses.[29] Furthermore, the normal mode character associated with the imaginary frequency was analysed to ensure that the correct TS was found. Reaction barriers are computed relative to the separated reactants. The molecular structures were illustrated using CYLview.[30]

3 | RESULTS AND DISCUSSION

3.1 | Competitive experiment

From the competitive experiment, the relative reactivity of the sodium borohydride reduction of 2-X-cyclohexanones (X=H, Cl, Br) and the stereoselectivity of the reaction to form *cis*- and *trans*-2-halocyclohexanol, measured by the amount of the corresponding alcohol formed, were investigated. The NMR experiments demonstrated that the parent ketones and *cis* halohydrins are the major components of the mixture at the end of the competitive experiment. As can be seen from Figure 1, the 2-halocyclohexanones are reduced in a higher extent compared with cyclohexanone (0.6%, 41.8% and 57.6% for X=H, Cl and Br, respectively), demonstrating that the α-halogens exert a strong effect on the reactivity in the given conditions, despite their larger steric effect compared with X=H. Furthermore, *cis*-2-halocyclohexanol is produced in larger amounts than the *trans* diastereoisomer (Figure 1), in agreement with previous experiments in the literature.[13,16,18] This asymmetric induction has been explained by several models in terms of intramolecular effects on the substrate, such as those mentioned above[3–9]; however, solvation effects cannot be neglected.[31] It is known that hydroxylic solvents play an important role on the kinetics of sodium borohydride reduction.[32] Therefore, in the following section, we investigate how the solvent affects the reactivity and stereoselectivity of the sodium borohydride reductions shown in Figure 1 using density functional theory computations. As the $NaBH_4$ reduction of both 2-halocyclohexanones showed similar results, only the 2-chlorocyclohexanone was further investigated computationally.

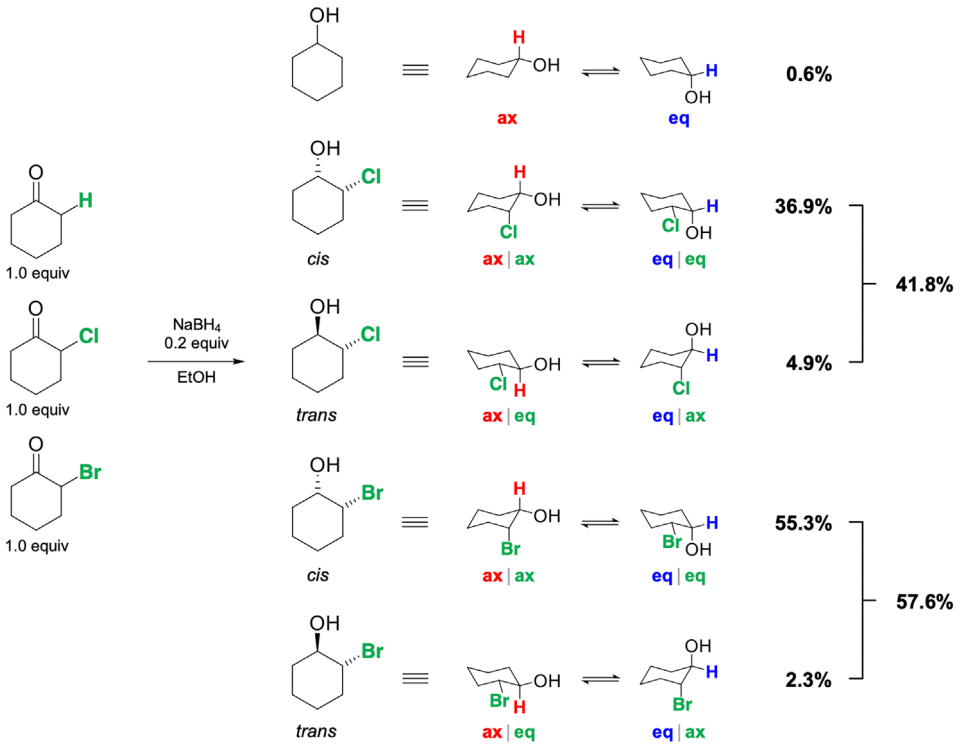

FIGURE 1 Competitive experiments of the sodium borohydride reduction of 2-X-cyclohexanones (X=H, Cl, Br) reaction pathways investigated herein that lead to the formation of the corresponding *cis* or *trans* halohydrins, and relative percentage of product formed determined by gas chromatography–flame ionization detection (GC–FID).

3.2 | Experimental versus theoretical trends

Geometries of the TSs and reaction barriers of the sodium borohydride reduction of 2-X-cyclohexanones (X=H, Cl), in both implicit and microsolvation (i.e., microsolvation = implicit and explicit solvation) using ethanol as solvent, are shown in Figure 2. Presumably, because of their highly polar character, all attempts to locate TSs in the gas phase failed. Note that all reaction pathways proceed via a late TS in which the C–H bond is nearly formed (r_{C-H} ~1.12–1.13 Å) in qualitative agreement with the mild reducing power of $NaBH_4$. Furthermore, our results show that the 2-chlorocyclohexanone (X=Cl) is always more reactive, that is, it has a lower reaction barrier than the unsubstituted cyclohexanone (X=H), in line with the reactivity trends obtained from the competitive experiments. For X=H, the hydride attack occurs preferentially to the axial face ($\mathbf{CH_{ax}}$) of the carbonyl group in both solvation models, as the Gibbs free energy barrier $\Delta G^{\ddagger}$ is at least 3 kcal mol^{-1} lower than that of the equatorial attack ($\mathbf{CH_{eq}}$). This is consistent with the well-known preferential axial attack of small hydrides (e.g., $LiAlH_4$ and $NaBH_4$) to 4-*tert*-butylcyclohexanone reported in the literature.[11,16,18] On the other hand, the stereoselective formation of the *cis* product for X=Cl (via $\mathbf{CH_{ax}}|\mathbf{CCl_{ax}}$ or $\mathbf{CH_{eq}}|\mathbf{CCl_{eq}}$; see Figure 1) can only be observed using the microsolvation model. Note that the explicit ethanol molecule induces geometrical changes in the solute; it especially prevents the complexation of Na^+ with equatorial chlorine, which may cause an artificial lowering of the $\mathbf{CH_{ax}}|\mathbf{CCl_{eq}}$ reaction barrier that leads to the formation of the *trans* diastereoisomer. Only by including an explicit ethanol molecule the experimentally observed stereoselectivities can be recovered. This highlights the importance of considering explicit solvation in modelling the reduction by sodium borohydride. The same trends can be observed in the electronic $\Delta E^{\ddagger}$ and Gibbs free energy $\Delta G^{\ddagger}$ barriers (red and blue in Figure 2, respectively). It is worth noting that, similarly to a hetero Diels–Alder scheme proposed by Domingo and Andrés,[33] the solvent molecule engages in a hydrogen bond with the solute to accelerate the reaction.

To understand the solvent effect on the computed reaction barriers shown in Figure 2, we take a step back and remove all solvent layers from the microsolvated TS geometries to analyse the intrinsic gas phase barriers, $\Delta E^{\ddagger}_{solute}$ (**X**). Then, we analyse the energy change associated with adding each solvent layer back individually. That is, going from the gas phase $\Delta E^{\ddagger}_{solute}$ (**X**) to only explicitly solvated barriers, $\Delta E^{\ddagger}_{solute}$ (**X**·EtOH), or to only implicitly solvated barriers, $\Delta E^{\ddagger}_{solution}$ (**X**), and then back to the microsolvated ones, $\Delta E^{\ddagger}_{solution}$ (**X**·EtOH), shown in Figure 2. This is schematically illustrated, and the

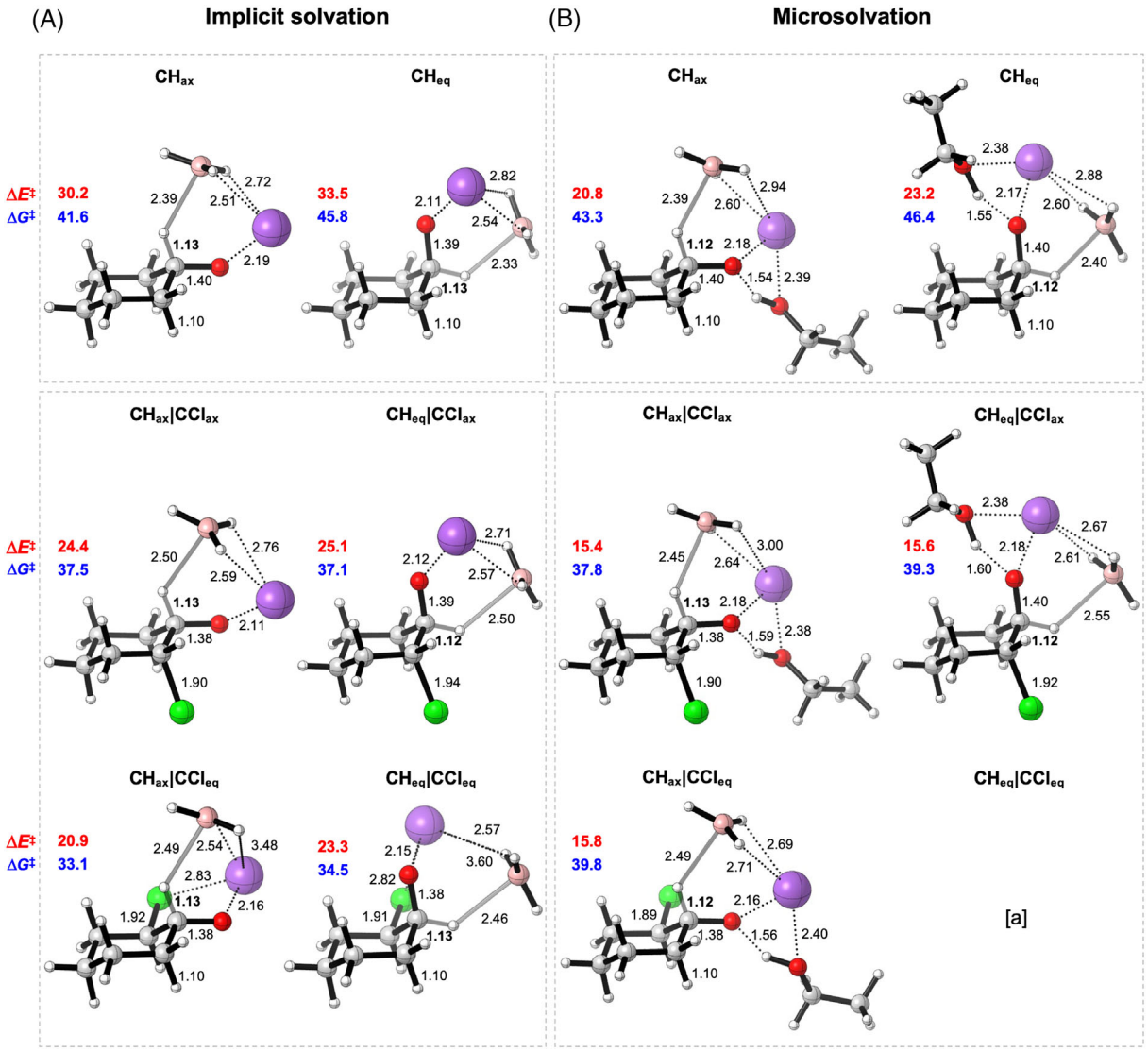

FIGURE 2 Geometries of the transition states (TS) (in Å, deg.; the forming carbon–hydride bond length is highlighted in bold) and electronic and Gibbs free energy barriers ($\Delta E^{\ddagger}$ in red and $\Delta G^{\ddagger}$ in blue, in kcal mol^{-1}) of the reaction pathways of sodium borohydride reduction of 2-X-cyclohexanones (X=H, Cl) in (A) implicit solvation (**X**) and (B) microsolvation (**X**·EtOH). Computed at conductor-like screening model (COSMO) (ethanol)-zeroth-order regular approximation (ZORA)-BLYP/TZ2P. [a] The **CH$_{eq}$**|**CCl$_{eq}$** TS could not be characterized in the microsolvation, therefore, **CH$_{eq}$**|**CCl$_{eq}$** conformer is considered to be obtained by ring interconversion of the **CH$_{ax}$**|**CCl$_{ax}$** conformer (see Figure 1).

results are collected in Table 1. Starting with the gas phase barriers—the $\Delta E^{\ddagger}_{solute}$ (**X**) entry—we observe again that X=Cl is more reactive than X=H. Furthermore, the stereoselectivity of the X=H reduction remains the same, that is, **CH$_{ax}$** is lower in energy than **CH$_{eq}$**. These results confirm the higher reactivity of 2-halocyclohexanones and the preference for the axial attack in the unsubstituted cyclohexanone as being intrinsic from the reactants, and not depending on the surrounding media. For X=Cl, on the other hand, the trends in stereoselectivity change, and $\Delta E^{\ddagger}_{solute}$ (**X**) increases along **CH$_{ax}$**|**CCl$_{eq}$** < **CH$_{eq}$**|**CCl$_{ax}$** < **CH$_{ax}$**|**CCl$_{ax}$**. That is, **CH$_{ax}$**|**CCl$_{ax}$**, the TS that leads to the *cis* product, which is produced in higher amounts in the competitive experiments, is actually the highest in energy. The same trend is observed if only explicit solvation is added back—the $\Delta E^{\ddagger}_{solute}$ (**X**·EtOH) entry. The interaction with an explicit solvent molecule decreases the reaction barriers in all cases; however, the relative trend remains the same, that is, $\Delta E^{\ddagger}_{solute}$ (**X**·EtOH) also increases along **CH$_{ax}$**|**CCl$_{eq}$** < **CH$_{eq}$**|**CCl$_{ax}$** < **CH$_{ax}$**|**CCl$_{ax}$**. Thus, the interaction with the explicit ethanol molecule alone does not change the stereoselectivity of hydride reduction of X=Cl.

TABLE 1 Effect of solvation on the energy barriers ($\Delta E^{\ddagger}$, in kcal mol^{-1}) of the sodium borohydride reduction of the 2-X-cyclohexanones (X=H, Cl) via axial and equatorial addition to the carbonyl group.[a]

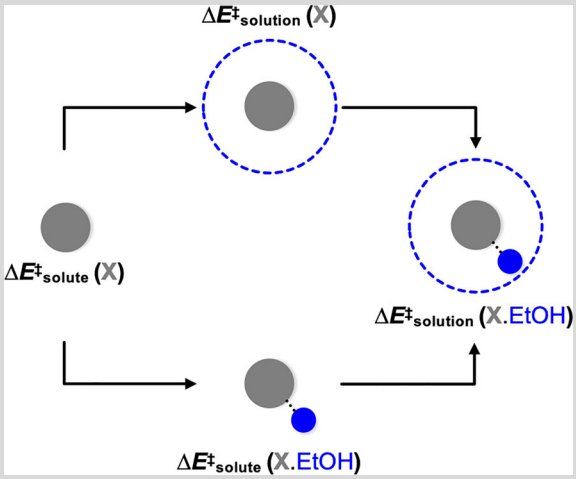

TS	$\Delta E^{\ddagger}_{solute}$ (X)[b]	$\Delta E^{\ddagger}_{solute}$ (X·EtOH)[c]	$\Delta E^{\ddagger}_{solution}$ (X)[d]	$\Delta E^{\ddagger}_{solution}$ (X·EtOH)[e]
CH_{ax}	22.6	1.1	30.8	20.8
CH_{eq}	23.4	2.2	34.7	23.2
CH_{ax}|CCl_{ax}	19.3	−2.1	25.5	15.4
CH_{ax}|CCl_{eq}	15.6	−5.0	25.0	15.8
CH_{eq}|CCl_{ax}	17.0	−3.2	26.5	15.6

Abbreviations: EtOH, ethanol; TS, transition state.
[a]Single-point computations on the microsolvation geometries.
[b]Gas phase barriers computed at ZORA-BLYP/TZ2P.
[c]Explicit solvation barriers computed at ZORA-BLYP/TZ2P.
[d]Implicit solvation barriers computed at COSMO (ethanol)-ZORA-BLYP/TZ2P.
[e]Microsolvation barriers computed at COSMO (ethanol)-ZORA-BLYP/TZ2P.

In turn, if only implicit ethanol solvent is taken into account—the $\Delta E^{\ddagger}_{solution}$ (**X**) entry—all reaction barriers increase, as the separate reactants are more stabilized by the solvent than the TSs.[34] This effect is slightly less pronounced for **CH_{ax}|CCl_{ax}**, which makes it very competitive with the other two TSs. For example, the difference in energy between **CH_{ax}|CCl_{ax}** and **CH_{ax}|CCl_{eq}** decreases from $\Delta\Delta E^{\ddagger}_{solute}$ (**X**) = 3.7 to $\Delta\Delta E^{\ddagger}_{solution}$ (**X**) = 0.5 kcal mol^{-1}. The stereoselectivity trends are completely reversed towards the *cis* product with the inclusion of the explicit solvent together with implicit solvation (i.e., microsolvation)—the $\Delta E^{\ddagger}_{solution}$ (**X**·OH) entry. Note that, at this point, any subtle energy difference is large enough to cause a trend shift in the already competitive $\Delta E^{\ddagger}_{solution}$ (**X**) barriers. Therefore, the largest effect observed with the inclusion of explicit ethanol molecules are the structural changes, especially the prevention of the $Na^{+}\cdots Cl$ complexation that underestimates the reaction barriers. Our results unravel the hitherto unsolved problem of theoretically reproducing the hydride reduction stereoselectivity of 2-substituted cyclohexanones with polar groups.[16,17]

4 | CONCLUSIONS

2-Halocyclohexanones (X=Cl, Br) are more reactive than unsubstituted cyclohexanone in the reduction reaction with $NaBH_4$ in ethanol, whereas an axial attack to the *axial* 2-X-cyclohexanone, leading to the *cis* product, controls the reaction stereoselectivity. These experimental results are recovered in quantum chemical calculations only when solvent effects are properly considered. We found that reaction barriers at COSMO (ethanol)-ZORA-BLYP/TZ2P in combination with one explicit ethanol molecule (microsolvation approach) were able to accurately estimate both the reactivity and stereoselectivity properties of this transformation. Coordination of the ethanol molecule to the reaction system via hydrogen bonding serves to impose a degree of geometrical rigidity that prevents the complexation of the equatorial halogen with the sodium atom, which we found leads to an underestimation of reaction barriers and a poor estimation of the reaction stereoselectivity. Therefore, we highlight that microsolvation is crucial to properly model a reaction pathway involving polar TSs.

ACKNOWLEDGEMENTS

The authors are thankful to the Coordenação de Aperfeiçoamento de Pessoal de Nível Superior—CAPES (funding code: 001), the Conselho Nacional de Desenvolvimento Científico e Tecnológico—CNPq (grant number: 306830/2021-3), the Fundação de Amparo à Pesquisa do Estado de Minas Gerais—FAPEMIG (grant number: APQ-00383/15), the Fundação de Amparo à Pesquisa do Estado de São Paulo—FAPESP (grant number: 2018/03910-1), the Fundo de Apoio ao Ensino, Pesquisa e Extensão—FAEPEX (grant number: 2466/20), and the Netherlands Organization for Scientific Research (NWO) for the financial support of this research. This work was carried out on the Dutch national e-infrastructure with the support of SURF Cooperative.

DATA AVAILABILITY STATEMENT

Data available in article supplementary material.

ORCID

Daniela Rodrigues Silva https://orcid.org/0000-0002-8191-7130
Lucas A. Zeoly https://orcid.org/0000-0003-2111-3904
Rodrigo A. Cormanich https://orcid.org/0000-0001-7659-1749
Trevor A. Hamlin https://orcid.org/0000-0002-5128-1004
Célia Fonseca Guerra https://orcid.org/0000-0002-2973-5321
Matheus P. Freitas https://orcid.org/0000-0002-7492-1801

REFERENCES

[1] B. W. Gung, *Chem. Rev.* **1999**, *99*, 1377.
[2] A. Mengel, O. Reiser, *Chem. Rev.* **1999**, *99*, 1191.
[3] D. J. Cram, F. A. A. Elhafez, *J. Am. Chem. Soc.* **1952**, *74*, 5828.
[4] D. J. Cram, K. R. Kopecky, *J. Am. Chem. Soc.* **1959**, *81*, 2748.
[5] J. W. Cornforth, R. H. Cornforth, K. K. Mathew, *J. Chem. Soc.* **1959**, *0*, 112.
[6] G. J. Karabatsos, *J. Am. Chem. Soc.* **1967**, *89*, 1367.
[7] M. Cherest, H. Felkin, N. Prudent, *Tetrahedron Lett.* **1968**, *18*, 2199.
[8] a) N. T. Anh, O. Eisenstein, *Nouv. J. Chim.* **1977**, *1*, 61; b) A. S. Cieplak, *J. Am. Chem. Soc.* **1981**, *103*, 4540.
[9] Y. D. Wu, J. A. Tucker, K. N. Houk, *J. Am. Chem. Soc.* **1991**, *113*, 5018.
[10] a) E. L. Eliel, M. N. Rerick, *J. Am. Chem. Soc.* **1960**, *82*, 1367; b) D. C. Wigfield, D. J. Phelps, *J. Org. Chem.* **1976**, *41*, 2396.
[11] S. R. Neufeldt, G. Jimenez-Oses, D. L. Comins, K. N. Houk, *J. Org. Chem.* **2014**, *79*, 11609.
[12] R. E. Rosenberg, W. J. Kelly, *J. Phys. Org. Chem.* **2015**, *28*, 47.
[13] O. O. Kolodiazhna, A. O. Kolodiazhna, O. I. Kolodiazhnyi, *Tetrahedron: Asymmetry* **2013**, *24*, 37.
[14] F. Yoshinaga, C. F. Tormena, M. P. Freitas, R. Rittner, R. J. Abraham, *J. Chem. Soc., Perkin Trans. 2* **2002**, *9*, 1494.
[15] G. Pattison, *Beilstein J. Org. Chem.* **2017**, *13*, 2915.
[16] R. E. Rosenberg, R. L. Abel, M. D. Drake, D. J. Fox, A. K. Ignatz, D. M. Kwiat, K. M. Schaal, P. R. Virkler, *J. Org. Chem.* **2001**, *66*, 1694.
[17] X. Deraet, T. Woller, R. Van Lommel, F. De Proft, G. Verniest, M. Alonso, *ChemistryOpen* **2019**, *8*, 788.
[18] R. T. Luibrand, I. R. Taigounov, A. A. Taigounov, *J. Org. Chem.* **2001**, *66*, 7254.
[19] a) G. te Velde, F. M. Bickelhaupt, E. J. Baerends, C. F. Guerra, S. J. A. van Gisbergen, J. G. Snijders, T. Ziegler, *J. Comput. Chem.* **2001**, *22*, 931; b) C. F. Guerra, J. G. Snijders, G. te Velde, E. J. Baerends, *Chem. Acc.* **1998**, *99*, 391; c) SCM. ADF2017.103, Theoretical Chemistry; Vrije Universiteit, Amsterdam, The Netherlands, http://www.scm.com
[20] a) A. D. Becke, *Phys. Rev. a* **1988**, *38*, 3098; b) C. Lee, W. Yang, R. G. Parr, *Phys. Rev. B* **1988**, *37*, 785.
[21] a) G. T. de Jong, M. Solà, L. Visscher, F. M. Bickelhaupt, *J. Chem. Phys.* **2004**, *121*, 9982; b) G. T. de Jong, D. P. Geerke, A. Diefenbach, F. M. Bickelhaupt, *J. Chem. Phys.* **2005**, *313*, 261; c) G. T. de Jong, D. P. Geerke, A. Diefenbach, M. Solà, F. M. Bickelhaupt, *J. Comput. Chem.* **2005**, *26*, 1006; d) G. T. de Jong, F. M. Bickelhaupt, *J. Phys. Chem. A* **2005**, *109*, 9685; e) P. Vermeeren, M. D. Tiezza, M. E. Wolf, M. E. Lahm, W. D. Allen, H. F. Schaefer III, T. A. Hamlin, F. M. Bickelhaupt, *Phys. Chem. Chem. Phys.* **2022**, *24*, 18028.
[22] a) E. van Lenthe, R. van Leeuwen, E. J. Baerends, J. G. Snijders, *Int. J. Quantum Chem.* **1996**, *57*, 281; b) E. van Lenthe, E. J. Baerends, J. G. Snijders, *J. Chem. Phys.* **1994**, *101*, 9783.
[23] E. van Lenthe, E. J. Baerends, *J. Comput. Chem.* **2003**, *24*, 1142.
[24] a) A. Klamt, G. Schüürmann, *J. Chem. Soc., Perkin Trans. 2* **1993**, *5*, 799; b) A. Klamt, *J. Phys. Chem.* **1995**, *99*, 2224; c) A. Klamt, V. Jonas, *J. Chem. Phys.* **1996**, *105*, 9972; d) C. C. Pye, T. Ziegler, *Theor Chem. Acc.* **1999**, *101*, 396.
[25] Y. Suzuki, D. Kaneno, S. Tomoda, *J. Phys. Chem. A* **2009**, *113*, 2578.
[26] M. Franchini, P. H. T. Philipsen, E. van Lenthe, L. Visscher, *J. Chem. Theory Comput.* **1994**, *2014*, 10.
[27] M. Franchini, P. H. T. Philipsen, L. Visscher, *J. Comput. Chem.* **1819**, *2013*, 34.
[28] a) S. Grimme, J. Antony, S. Ehrlich, H. Krieg, *J. Chem. Phys.* **2010**, *132*, 154104; b) S. Grimme, S. Ehrlich, L. Goerigk, *J. Comput. Chem.* **2011**, *32*, 1456.
[29] a) A. Bérces, R. M. Dickson, L. Fan, H. Jacobsen, D. Swerhone, T. Ziegler, *Comput. Phys. Commun.* **1997**, *100*, 247; b) H. Jacobsen, A. Bérces, D. P. Swerhone, T. Ziegler, *Comput. Phys. Commun.* **1997**, *100*, 263; c) S. K. Wolff, *Int. J. Quantum Chem.* **2005**, *104*, 645.
[30] C. Y. Legault, *CYLview, 1.0b; Université de Sherbrooke*, Sherbrooke, QC, Canada **2009** http://www.cylview.org
[31] P. Song, M. Ruan, X. Sun, Y. Zhang, W. Xu, *J. Phys. Chem. B* **2014**, *118*, 10224.

[32] a) D. C. Wigfield, F. W. Gowland, *J. Org. Chem.* **1977**, *42*, 1108; b) D. C. Wigfield, *Tetrahedron* **1979**, *35*, 449.
[33] L. R. Domingo, J. Andrés, *J. Org. Chem.* **2003**, *68*, 8662.
[34] T. A. Hamlin, B. van Beek, L. P. Wolters, F. M. Bickelhaupt, *Chem. – Eur. J.* **2018**, *24*, 5927.

SUPPORTING INFORMATION

Additional supporting information can be found online in the Supporting Information section at the end of this article.

How to cite this article: D. Rodrigues Silva, L. A. Zeoly, P. Vermeeren, R. A. Cormanich, T. A. Hamlin, C. Fonseca Guerra, M. P. Freitas, *J Phys Org Chem* **2023**, *36*(10), e4556. https://doi.org/10.1002/poc.4556